

Distributed Global Optimal Coverage Control in Multi-agent Systems: Known and Unknown Environments^{*}

Mohammadhasan Faghihi^a, Meysam Yadegar^a,
Mohammadhosein Bakhtiaridoust^a, Nader Meskin^b, Javad Sharifi^a, Peng Shi^c,

^a*Department of Electrical and Computer Engineering, Qom University of Technology, Qom, Iran*

^b*Department of Electrical Engineering, Qatar University, Doha, Qatar*

^c*School of Electrical and Electronic Engineering, University of Adelaide, Adelaide, SA 5005, Australia*

Abstract

This paper introduces a novel approach to solve the coverage optimization problem in multi-agent systems. The proposed technique offers a solution that not only achieves the global optimality in the agents configuration but also effectively handles the issue of agents remaining stationary in regions void of information. The proposed approach leverages a novel cost function for optimizing the agents coverage and the cost function eventually aligns with the conventional Voronoi-based cost function. Theoretical analyses are conducted to assure the asymptotic convergence of agents towards the optimal configuration. A distinguishing feature of this approach lies in its departure from the reliance on geometric methods that are characteristic of Voronoi-based approaches; hence can be implemented more simply. Remarkably, the technique is adaptive and applicable to various environments with both known and unknown information distributions. Lastly, the efficacy of the proposed method is demonstrated through simulations, and the obtained results are compared with those of Voronoi-based algorithms.

Key words: Informative Coverage; Density Function; Voronoi Algorithm; Multi-agent; Global Optimality; Known-Unknown environment.

1 Introduction

A multi-agent system is a collection of autonomous agents that interact with each other and their environment to achieve individual and/or collective goals [12, 17]. These agents can be robots, vehicles, drones, or any other entities capable of making decisions and taking actions [13]. Multi-agent systems find applications in various fields such as inspection of various environments [9], path planning of autonomous underwater robots [29, 35], multi-unmanned aerial vehicles for dynamic wildfire tracking [19], city surveillance tasks [16], and robot vacuum cleaning tasks [18].

One of the fundamental challenges in multi-agent systems is the coverage control problem [10, 27, 28]. Coverage control involves distributing agents in such a way that they collectively explore and monitor a given environment efficiently and effectively. In other words, the objective is to position the agents within an environment in such a way that they can gather the maximum amount of data sources or information. Additionally, this positioning strategy aims

^{*} This paper was not presented at any IFAC meeting.
Corresponding author Nader Meskin.

Email addresses: faghihi.mh@qut.ac.ir (Mohammadhasan Faghihi), yadegar@qut.ac.ir (Meysam Yadegar), bakhtiaridoust.mh@qut.ac.ir (Mohammadhosein Bakhtiaridoust), nader.meskin@qu.edu.qa (Nader Meskin), sharifi@qut.ac.ir (Javad Sharifi), peng.shi@adelaide.edu.au (Peng Shi).

to prevent unnecessary overlap between agents' coverage areas. In order to formulate the coverage control problem, the information in the environment is modeled by a mathematical function called the *density function* [33], and the desired agents configuration metric is modeled by minimizing a function named the *cost function*. The solution to this global minimization problem is called *global optimum configuration* [33].

The coverage environment can either be known or unknown in terms of agents' knowledge of the density function. In a known environment, the density function of each point in the environment is known for every agent, and the coverage control problem involves arranging the positions of agents to optimally sense regions of interest based on some specific cost functions. However, in an unknown environment, the density function is not priorly known for each agent, and agents, therefore, must learn the density function of the environment by identifying interesting regions and gathering information about them during their movement. Moreover, the non-convex nature of the metric used to assess the effectiveness of agents' positions in covering a designated area adds complexity to the optimization of the coverage problem.

In general, two primary approaches are employed to address the coverage problem: the greedy-evolutionary and Voronoi-based methods [30]. The former combine elements of both greedy algorithms, which make locally optimal choices at each step, and evolutionary algorithms, which mimic natural selection processes to find better solutions over time. They aim to iteratively improve coverage by selecting and evolving agent positions. In [30], a greedy algorithm is employed with two performance bounds using partial and greedy curvature to construct the coverage component of the objective function. In [14], a novel particle swarm optimization (PSO) technique is used to address the sensor deployment problem, and in [25], a genetic algorithm is developed for the coverage path planning of unmanned aerial vehicles (UAVs) while minimizing their energy consumption. Although these approaches may yield nearly optimal solutions, the computational cost is prohibitively high, making them inappropriate for online and real-time applications.

On the other hand, Voronoi-based methods [7, 23, 36], make a trade-off between potential optimality and efficiency, opting to prioritize efficiency over achieving the absolute best solution. This approach is particularly valuable in scenarios where the real-time performance or the scalability of the solution is crucial. In this method, a distinctive two-step procedure is employed. First, the environment is partitioned into to distinct and separate subareas, i.e., Voronoi cells, where a group of agents is allocated to each cells, setting the stage for active sensing tasks. Following this assignment, mobile agents are systematically guided to their respective optimal positions based on the distribution of information within their cells.

A Lloyd approach based on Voronoi partition was first adapted in [7] for the optimal coverage problem in autonomous vehicle networks performing distributed sensing tasks. In [23], a controller is proposed that utilizes parameter adaptation to address coverage tasks in unknown sensory environments, while also incorporating a consensus term within the parameter adaptation law to propagate sensory information among the robots in the network. In [36], a Bayesian prediction-based coverage control strategy is presented for a multi-agent system where it takes into account noise and is capable of approximating time-varying density functions. In [4], the Gaussian process upper confidence bound (GP-UCB) algorithm is combined with the Lloyd control algorithm to achieve coverage in an unknown domain. The work in [37] introduces an adaptive spatial estimation algorithm for the mobile sensor network with the main aim of estimating the density function and guiding the sensors to their optimal positions. The work described in [24] proposes a distributed motion control algorithm in which the robots proceed asynchronously with dead-zone-based robustification. In [3], the informative coverage algorithm is proposed by considering the non-holonomic limitations and the unknown dynamics of the mobile robots. A coverage method for unicycle robots is also suggested in [31], while taking outside disturbance into account. A time-varying density function was used to describe the time cost metric of a robot network with an input disturbance in [32] for a dynamic environment. In [6], taking into account the input and state constraints, a method based on the combination of predictive model control and Voronoi coverage control is presented. The research conducted in [26] suggests an online adaptive distributed controller that relies on implementing a Voronoi-based cost function using gradient descent for coverage tasks. In [2], a novel team-based strategy is presented that allows the formation of several teams of agents within the coverage control framework with the heterogeneity in their embedded communication capabilities or dynamics. A distributed, self-triggered control strategy for centroidal Voronoi coverage control is presented in [20] where the agent sampling or communication instants are reduced without affecting the performance of the mobile sensor network.

While the efficiency of this approach proves beneficial for scenarios demanding real-time performance, it does encounter an issue with the localized optimality of the solution. Therefore, the optimality of the final configuration of the agents heavily depends on their initial positions. Moreover, if an agent is situated within a Voronoi partition that

Table 1
Summary of the literature review on coverage control

Ref.	Optimality Scope	Separated Information Area Handling	Non-reliance on Geometric Computations	Unknown Environment Coverage
[2, 6, 7, 23, 32]	Local	\times	\times	\times
[3, 4, 24, 31, 36, 37]	Local	\times	\times	\checkmark
[26]	Local	\checkmark	\times	\checkmark
This paper	Global	\checkmark	\checkmark	\checkmark

lacks any sensory information, the agent will remain stationary indefinitely. This circumstance results in inefficient resource allocation for environmental coverage.

In this paper, based on the above discussion, we introduce an innovative distributed coverage technique which aims at resolving the challenges outlined earlier. Our approach not only establishes the global optimality of the final agent configuration but also addresses the issue of agents remaining stationary when surrounded by information voids. Specifically, we reframe the problem by formulating the optimization of agent composition using a novel metric. This metric progressively converges to the conventional Voronoi-based cost function as time extends towards infinity. In our analysis, we demonstrate the asymptotic convergence of agents towards the global optimum configuration. Notably, our method is versatile, applicable to both known and unknown environments featuring separated information areas. Furthermore, unlike Voronoi-based methods, our presented approach circumvents the need for geometric techniques, such as determining Voronoi diagram partitioning edges. As a result, our method can be implemented with greater simplicity. A summary of the literature review and a comparison between our method and other Voronoi-based approaches are presented in TABLE 1.

Overall, the contributions of this paper can be summarized as follows:

- This paper introduces a new approach for coordinating a group of agents to achieve comprehensive coverage of an area. The proposed technique ensures that the final configuration of agents is globally optimal where the agents' asymptotic convergence to global optimum is proven. Hence, the proposed method is not sensitive to the initial configuration of agents.
- In contrast to the Voronoi-based approaches, where agents can get stuck in areas without information, the proposed method adeptly navigates agents through such areas, preventing them from remaining stationary and ensuring more effective coverage.
- The proposed technique can be applied to both known and unknown environments with arbitrary density function and separated information areas. This adaptability makes the method versatile and usable in a wide range of scenarios.
- Unlike traditional methods that require complex geometric calculations for Voronoi diagram edges, the proposed technique does not rely on such techniques; hence leads to simpler implementation.

The rest of the paper is organized as follows: The notations and preliminaries are described in Section 2. Section 3 addresses the problem formulation. Section 4 presents the proposed coverage control algorithm for both known and unknown environments. In Section 5, using several simulation scenarios, the performance of the proposed method is evaluated, and a comparison with the Voronoi-based method is conducted. Finally, Section 6 concludes the paper.

2 Notations and Preliminaries

In order to show the problem addressed in this paper, the conventional representation of required variables such as matrices and vectors is presented in bold. \mathbb{R} and $\mathbb{R}_{\geq 0}$, respectively, stand for the real number field and the set of non-negative real numbers. The set of $n \times 1$ real column vectors is denoted by \mathbb{R}^n and the set of $n \times m$ real matrices is denoted by $\mathbb{R}^{n \times m}$. Furthermore, \mathbf{I}_n represents $n \times n$ identity matrix, $\mathbf{0}_{n \times m}$ represents $n \times m$ zero matrix, $\mathbf{1}_{n \times m}$ represents $n \times m$ one matrix, $(\cdot)^T$ represents transpose, $|\cdot|$ is the absolute value, and $\|\cdot\|$ is the Euclidean norm.

The directed graph $\mathcal{G} = (\mathcal{V}, \mathcal{E})$, where $\mathcal{V} = \{v_1, v_2, \dots, v_n\}$ is the collection of agent indexes and $\mathcal{E} \in \mathcal{V} \times \mathcal{V}$ is the set of edges connecting different agents, serves as a representation of the communication topology among n agents. If $(v_i, v_j) \in \mathcal{E}$, it means that the agent j and the agent i are neighbors and that the agent j can obtain information from the agent i . The presumption is that self edges, i.e., (v_i, v_i) , is not permitted. Suppose, a function $l : \mathcal{V} \times \mathcal{V} \rightarrow \mathbb{R}$ such that $l_{i,j} > 0$ if $(v_i, v_j) \in \mathcal{E}$, and $l_{i,j} = 0$ if $(v_i, v_j) \notin \mathcal{E}$, where $l_{i,j} \geq 0$ represents the strength of communication between agents i and j .

Additionally, $\mathbf{L} \in \mathbb{R}^{n \times n}$ is the system's weighted graph Laplacian and is defined as

$$\mathbf{L}_{i,j} = \begin{cases} -l_{i,j}, & \text{for } i \neq j, \\ \sum_{j=1}^n l_{i,j}, & \text{for } i = j. \end{cases} \quad (1)$$

If the agents network is connected, the graph's Laplacian is positive semi-definite, and it has precisely one zero eigenvalue with the associated eigenvector of $\mathbf{1}_{n \times 1}$. Furthermore, $\kappa(\cdot)$ is the heavy side function and is defined as follows:

$$\kappa(c) = \begin{cases} 1, & \text{for } c > 0, \\ 0, & \text{for } c \leq 0. \end{cases} \quad (2)$$

In addition, $\delta(\cdot)$ is the derivative of $\kappa(\cdot)$, and $\delta(x) = 0$, $\forall x \neq 0$, and $\int \delta(x)dx = 1$.

3 Problem Formulation

In the following, it is assumed that there exist n agents in a bounded and convex environment denoted by $\mathbf{Q} \subseteq \mathbb{R}^N$. An arbitrary point in \mathbf{Q} is denoted by \mathbf{q} . Furthermore, the position of each agent in the environment at time t is represented by $\mathbf{p}_i(t) \in \mathbf{Q}$, $i = 1, \dots, n$.

Definition 1 (Voronoi partition) *The Voronoi partition of the environment \mathbf{Q} generated by the i th agent at time t named as the generator point of Voronoi is defined as [7]:*

$$V_i(t) = \{\mathbf{q} \in \mathbf{Q} \mid \|\mathbf{q} - \mathbf{p}_i(t)\| \leq \|\mathbf{q} - \mathbf{p}_j(t)\|, \quad j = 1, \dots, n, j \neq i\}. \quad (3)$$

It is assumed that each agent is able to compute its Voronoi partition, based on its location and other agents locations. Furthermore, the density function of the available information in the environment is defined as follows [1]:

Definition 2 (Density function) *The density function is defined as $\phi : \mathbf{Q} \rightarrow \mathbb{R}_{\geq 0}$ with the following property:*

$$0 < \int_{\mathbf{Q}} \phi(\mathbf{q})d\mathbf{q} \leq \eta < \infty, \quad (4)$$

where the larger values of $\phi(\mathbf{q})$ correspond to more important areas.

Definition 3 (Known environment) *A known environment is an environment where the agent knows the value of $\phi(\mathbf{q})$ for each $\mathbf{q} \in \mathbf{Q}$. In fact, the agent does not require to measure information using the relevant sensors.*

Definition 4 (Unknown environment) *The unknown environment is the environment where the value of $\phi(\mathbf{q})$, $\forall \mathbf{q} \in \mathbf{Q}$, is not priorly known for each agent, and consequently each agent needs to measure or estimate it by its relevant sensors.*

Definition 5 (Zero information area) *A subset $\Omega \subset \mathbf{Q}$ is called a zero information area if $\phi(q) = 0, \forall q \in \Omega$.*

Definition 6 (Separated information area) *\mathbf{Q} is called an environment with separated information areas if it can be partitioned into compact sets $\mathbf{A}_l, l = 1, 2, \dots, l_n$, and contains at least one zero information area.*

Conventionally, the converge problem is modeled based on the Voronoi diagram and the following cost function [7,23]:

$$H(\mathbf{P}(t)) \triangleq \frac{1}{2} \sum_{i=1}^n \int_{V_i(t)} \|\mathbf{q} - \mathbf{p}_i(t)\|^2 \phi(\mathbf{q})d\mathbf{q}, \quad (5)$$

such that

$$H(\mathbf{P}(t)) \geq H_{\min} > 0, \quad t \geq 0, \quad (6)$$

where H_{\min} is lower bound of H , and $\mathbf{P}(t) \triangleq \{\mathbf{p}_1(t), \dots, \mathbf{p}_n(t)\}$.

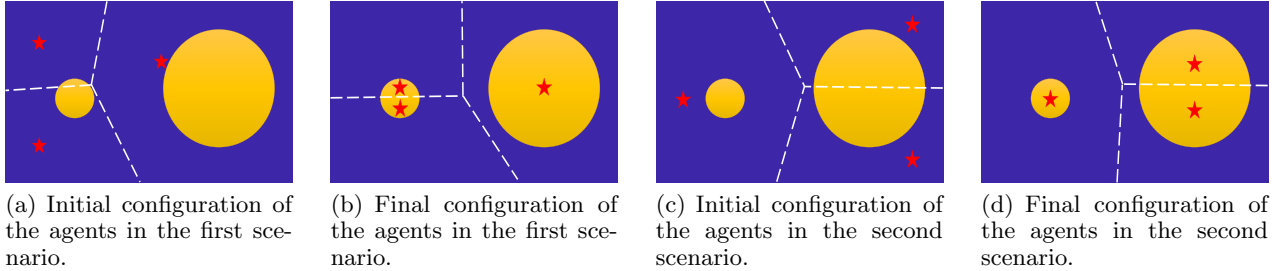


Fig. 1. The effect of the initial conditions on the final configuration in Voronoi-based methods. Yellow regions represent areas with information, while red stars indicate agents' positions. The white dash lines indicates the Voronoi-cells edges.

Definition 7 (Globally optimal coverage configuration) An agent network is said to be in the globally optimal coverage configuration if every agent is positioned at \mathbf{p}_i^* such that $H(\mathbf{P}^*) = H_{\min}$, where $\mathbf{P}^* \triangleq \{\mathbf{p}_1^*, \dots, \mathbf{p}_n^*\}$.

Assume the agents' locations obey a first-order dynamical behavior described by

$$\dot{\mathbf{p}}_i(t) = \mathbf{u}_i(t), \quad i = 1, \dots, n, \quad (7)$$

where $\mathbf{u}_i(t) \in \mathbb{R}^N$ is the control input.

In order to find the minimum value of cost function for calculating the position of each agent, the gradient descent method is used as follows [7, 22]:

$$\begin{aligned} \dot{\mathbf{p}}_i(t) &= -k_i \frac{\partial H(\mathbf{P}(t))}{\partial \mathbf{p}_i(t)} = k_i \int_{V_i(t)} (\mathbf{q} - \mathbf{p}_i(t)) \phi(\mathbf{q}) d\mathbf{q} \\ &= k_{\text{prop}_i}(t) (\mathbf{C}_{V_i}(t) - \mathbf{p}_i(t)), \end{aligned} \quad (8)$$

where k_i and $k_{\text{prop}_i}(t) \triangleq k_i \int_{V_i(t)} \phi(\mathbf{q}) d\mathbf{q}$ are positive gains and $\mathbf{C}_{V_i}(t)$ is the centroid of a Voronoi partition obtained as follows:

$$\mathbf{C}_{V_i}(t) = \frac{\int_{V_i(t)} \mathbf{q} \phi(\mathbf{q}) d\mathbf{q}}{\int_{V_i(t)} \phi(\mathbf{q}) d\mathbf{q}}. \quad (9)$$

Equation (8) implies that each agent is moving towards the centroid of its Voronoi partition.

One of the major drawbacks of utilizing the Voronoi-based methods given by (8) and (9) to position agents appropriately is the high sensitivity of the final configuration to the initial placement of the agents. For instance, the initial configurations shown in Fig. 1(a) and Fig. 1(c) led to two different final configurations shown in Fig. 1(b) and Fig. 1(d), respectively. It is clear from (5) that these two configurations have different cost values.

The problem gets even worse when dealing with large environment that contain zero information areas as Voronoi partitions. In this case, the control input of the relevant agent can not be computed using (9). This issue is also evident in methodologies like those presented in [2, 7, 23], as well as clustering-based approaches such as [34]. This problem is rooted in the fact that the agents are confined to their own Voronoi partition and cannot leverage the available information in other Voronoi partitions. To circumvent this problem, first the function (5) is reformulated based on the whole environment as follows:

$$H(\mathbf{P}(t)) = \frac{1}{2} \sum_{i=1}^n \int_{\mathbf{Q}} h_i(\mathbf{q}, \mathbf{P}(t)) \|\mathbf{q} - \mathbf{p}_i(t)\|^2 \phi(\mathbf{q}) d\mathbf{q}, \quad (10)$$

where

$$h_i(\mathbf{q}, \mathbf{P}(t)) = \begin{cases} 1, & \text{if } \|\mathbf{q} - \mathbf{p}_i(t)\| \leq \|\mathbf{q} - \mathbf{p}_j(t)\|, \quad \forall j, \\ 0, & \text{otherwise.} \end{cases} \quad (11)$$

Comparing (5) and (10), the Voronoi partition is modeled by $h_i(\mathbf{q}, \mathbf{P}(t))$, $i = 1, \dots, n$. Using (10), each agent utilizes the information from its Voronoi partition to compute its control input, as previously mentioned. However, our

objective is to develop an alternative cost function capable of leveraging comprehensive environmental information to address the aforementioned issues. It is important to highlight that in both the Voronoi-based method and our proposed framework, every agent must have knowledge of the positions of all agents. Furthermore, in scenarios where the density function is unknown, our method performs distributed estimation of environmental information and subsequently optimizes the cost function to determine the control input.

4 Proposed Method

In this section, the proposed global optimal coverage configuration algorithm is presented for two cases, namely known and unknown environments. For this purpose, first, some definitions and lemmas are needed to be introduced.

Definition 8 (Ranking function) *The agent i ranking function $R_i : \mathbf{Q} \times \mathbf{P} \rightarrow \{0, \dots, n-1\}$ is defined as follows:*

$$R_i(\mathbf{q}, \mathbf{P}(t)) = \sum_{l=1}^n \kappa(\|\mathbf{q} - \mathbf{p}_i(t)\| - \|\mathbf{q} - \mathbf{p}_l(t)\|), \quad i = 1, \dots, n. \quad (12)$$

Based on the definition of $R_i(\mathbf{q}, \mathbf{P}(t))$, each agent i at time $t \geq 0$ assigns a rank $R_i(\mathbf{q}, \mathbf{P}(t))$ between 0 to $n-1$ to all the points in the environment, where the points that the closest agent is the i -th agent receive (0)-rank, i.e. $R_i(\mathbf{q}, \mathbf{P}(t)) = 0$, the points that the second closest agent is the i -th agent receive (1)-rank, i.e. $R_i(\mathbf{q}, \mathbf{P}(t)) = 1$, and the points that the farthest agent is the i -th agent receive $(n-1)$ -rank, i.e. $R_i(\mathbf{q}, \mathbf{P}(t)) = n-1$.

Lemma 1 *Based on the definition of $R_i(\mathbf{q}, \mathbf{P}(t))$ given by (12), the following equation holds:*

$$\frac{\partial R_j(\mathbf{q}, \mathbf{P}(t))}{\partial \mathbf{p}_i(t)} = 0, \quad i, j \in \{1, \dots, n\}. \quad (13)$$

Proof. Using (12), for $i \neq j$ one can write:

$$\frac{\partial R_j(\mathbf{q}, \mathbf{P}(t))}{\partial \mathbf{p}_i(t)} = \frac{\partial(\|\mathbf{q} - \mathbf{p}_j(t)\| - \|\mathbf{q} - \mathbf{p}_i(t)\|)}{\partial \mathbf{p}_i(t)} \delta(\|\mathbf{q} - \mathbf{p}_j(t)\| - \|\mathbf{q} - \mathbf{p}_i(t)\|).$$

and since $\delta(\|\mathbf{q} - \mathbf{p}_j(t)\| - \|\mathbf{q} - \mathbf{p}_i(t)\|) = 0$ and hence (13) is obtained. For $i = j$, we have:

$$\frac{\partial R_i(\mathbf{q}, \mathbf{P}(t))}{\partial \mathbf{p}_i(t)} = \sum_{l=1}^n \frac{\partial(\|\mathbf{q} - \mathbf{p}_i(t)\| - \|\mathbf{q} - \mathbf{p}_l(t)\|)}{\partial \mathbf{p}_i(t)} \delta(\|\mathbf{q} - \mathbf{p}_i(t)\| - \|\mathbf{q} - \mathbf{p}_l(t)\|).$$

For $i \neq l$, we have $\delta(\|\mathbf{q} - \mathbf{p}_i(t)\| - \|\mathbf{q} - \mathbf{p}_l(t)\|) = 0$ and for $i = l$, the first term in the above summation is zero which leads to (13). \square

In this work, the following cost function is introduced:

$$\hat{H}(t, \mathbf{P}(t)) \triangleq \frac{1}{2} \sum_{i=1}^n \int_{\mathbf{Q}} h_\lambda(t, R_i(\mathbf{q}, \mathbf{P}(t))) \|\mathbf{q} - \mathbf{p}_i(t)\|^2 \phi(\mathbf{q}) d\mathbf{q}, \quad (14)$$

where

$$h_\lambda(t, R_i(\mathbf{q}, \mathbf{P}(t))) = \exp\left\{\frac{-R_i(\mathbf{q}, \mathbf{P}(t))}{\lambda(t)}\right\}, \quad (15)$$

and $\lambda(t) : \mathbb{R}_{\geq 0} \rightarrow \mathbb{R}_{\geq 0}$ where $\lim_{t \rightarrow \infty} \lambda(t) = 0$.

Remark 1 The choice of the parameter $\lambda(t)$ can be of great importance. Exponential functions, such as $\lambda(t) = \lambda_s \alpha^{-\lambda_f t}$ where $\lambda_s, \lambda_f > 0$, and $\alpha > 1$, are often considered due to their mathematical simplicity and their ability to model various types of dynamics. Specifically, λ_s represents the initial growth rate or scaling factor. Additionally, α serves as another vital parameter, impacting the exponential function's shape and behavior, while λ_f controls the rate of exponential growth or decay over time.

Remark 2 Unlike $h_i(\cdot)$ given by (11) which has a binary value, $h_\lambda(\cdot)$ can have any value in the range of $[0, 1]$. According to Definition 8, the closest agent to the point $\mathbf{q} \in \mathbf{Q}$ gets the maximum value of $h_\lambda(\cdot)$, and the rest of the agents get $0 < h_\lambda < 1$.

Lemma 2 Considering (10) and (14), for any fixed configuration of agents $\mathbf{P} \triangleq \{\mathbf{p}_1, \dots, \mathbf{p}_n\}$, the following equation holds:

$$\lim_{t \rightarrow \infty} \hat{H}(t, \mathbf{P}) = H(\mathbf{P}). \quad (16)$$

Proof. According to the definition of $\lambda(t)$ given by (15), we can deduce that $\lambda(t) \rightarrow 0$ as $t \rightarrow \infty$. Moreover, based on Definition 8, $R_i(\mathbf{q}, \mathbf{P}) = 0$, if $\|\mathbf{q} - \mathbf{p}_i\| \leq \|\mathbf{q} - \mathbf{p}_j\|, \forall j$. Hence,

$$\lim_{t \rightarrow \infty} h_\lambda(t, R_i(\mathbf{q}, \mathbf{P})) = \begin{cases} 1, & \text{if } \|\mathbf{q} - \mathbf{p}_i\| \leq \|\mathbf{q} - \mathbf{p}_j\|, \forall j, \\ 0, & \text{otherwise,} \end{cases} \quad (17)$$

therefore, using (11), we have

$$\lim_{t \rightarrow \infty} h_\lambda(t, R_i(\mathbf{q}, \mathbf{P})) = h_i(\mathbf{q}, \mathbf{P}), \quad (18)$$

which leads to (16). \square

For ease of notation, we denote $h_\lambda(t, R_i)$ and $\hat{H}(t)$ for $h_\lambda(t, R_i(\mathbf{q}, \mathbf{P}(t)))$ and $\hat{H}(t, \mathbf{P}(t))$, respectively.

4.1 Known Environment

In this section, a known environment is considered and a control signal for each agent is designed such that the proposed cost function $\hat{H}(\cdot)$ introduced by (14) is globally minimized. As proved in Lemma 2, $\hat{H}(\cdot) \rightarrow H(\cdot)$ as $t \rightarrow \infty$. Hence, using the proposed control input, the conventional cost function is globally minimized and the globally optimal coverage configuration can be obtained. For this purpose, similar to the Voronoi-based algorithms, the gradient descent method is used to update the position of each agent as follows:

$$\mathbf{u}_i(t) = -\epsilon \frac{\partial \hat{H}(t)}{\partial \mathbf{p}_i(t)}, \quad i = 1, \dots, n, \quad (19)$$

where ϵ is a positive scalar gain. The following lemma shows the calculation of the right-hand side of (19).

Lemma 3 Consider the proposed cost function given by (14). The following equation holds:

$$\frac{\partial \hat{H}(t)}{\partial \mathbf{p}_i(t)} = - \int_{\mathbf{Q}} h_\lambda(t, R_i) (\mathbf{q} - \mathbf{p}_i(t)) \phi(\mathbf{q}) d\mathbf{q}. \quad (20)$$

Proof. According to (14), we can write

$$\frac{\partial \hat{H}(t)}{\partial \mathbf{p}_i(t)} = \frac{1}{2} \sum_{j=1}^n \int_{\mathbf{Q}} \left[h_\lambda(t, R_i) \frac{\partial (\|\mathbf{q} - \mathbf{p}_j(t)\|^2)}{\partial \mathbf{p}_i(t)} + \frac{\partial h_\lambda(t, R_i)}{\partial \mathbf{p}_i(t)} \|\mathbf{q} - \mathbf{p}_j(t)\|^2 \right] \phi(\mathbf{q}) d\mathbf{q}. \quad (21)$$

Using the chain rule and some manipulations, the following is obtained.

$$\frac{\partial \hat{H}(t)}{\partial \mathbf{p}_i(t)} = - \int_{\mathbf{Q}} h_{\lambda}(t, R_i)(\mathbf{q} - \mathbf{p}_i(t))\phi(\mathbf{q})d\mathbf{q} + \frac{1}{2} \sum_{j=1}^n \int_{\mathbf{Q}} \frac{\partial h_{\lambda}(t, R_j)}{\partial R_j} \frac{\partial R_j(\mathbf{q}, \mathbf{P}(t))}{\partial \mathbf{p}_i(t)} \|\mathbf{q} - \mathbf{p}_i(t)\|^2 \phi(\mathbf{q})d\mathbf{q}. \quad (22)$$

Based on Lemma 1, the second term of the right-hand side of (22) is vanished and the proof is completed. \square

Using this lemma and (20), the control law of the proposed method is obtained as follows:

$$\mathbf{u}_i(t) = \epsilon W_i(t), \quad (23)$$

where

$$\mathbf{W}_i(t) \triangleq \int_{\mathbf{Q}} h_{\lambda}(t, R_i)(\mathbf{q} - \mathbf{p}_i(t))\phi(\mathbf{q})d\mathbf{q}. \quad (24)$$

The following lemma gives some facts about $\mathbf{W}_i(t)$.

Lemma 4 $\mathbf{W}_i(t)$ and $\frac{\partial \mathbf{W}_i(t)}{\partial \mathbf{p}_i(t)}$ are bounded and

$$\frac{\partial \mathbf{W}_i(t)}{\partial \mathbf{p}_i(t)} = - \int_{\mathbf{Q}} h_{\lambda}(t, R_i)\phi(\mathbf{q})d\mathbf{q}\mathbf{I}_N. \quad (25)$$

Proof. Since \mathbf{Q} is a bounded environment, and $h_{\lambda}(\cdot)$ and $\phi(\cdot)$ are bounded, hence $\mathbf{W}_i(t)$ is also bounded. Using the chain rule, we have

$$\frac{\partial \mathbf{W}_i(t)}{\partial \mathbf{p}_i(t)} = \int_{\mathbf{Q}} \left[\frac{\partial h_{\lambda}(t, R_i)}{\partial R_i} \frac{\partial R_i(\mathbf{q}, \mathbf{P}(t))}{\partial \mathbf{p}_i(t)} (\mathbf{q} - \mathbf{p}_i(t))^{\text{T}} - h_{\lambda}(t, R_i)\mathbf{I}_N \right] \phi(\mathbf{q})d\mathbf{q}. \quad (26)$$

Based on Lemma 1, (25) is obtained. Since $h_{\lambda}(t, R_i) \in [0, 1]$, then

$$0 < \int_{\mathbf{Q}} h_{\lambda}(t, R_i)\phi(\mathbf{q})d\mathbf{q} \leq \int_{\mathbf{Q}} \phi(\mathbf{q})d\mathbf{q} < \eta. \quad (27)$$

Therefore, $\frac{\partial \mathbf{W}_i(t)}{\partial \mathbf{p}_i(t)}$ is bounded. \square

Lemma 5 The proposed cost function given by (14) is a convex function.

Proof. A function is convex if its Hessian matrix is positive semidefinite [5]. Therefore, we just need to show that the Hessian matrix of $\hat{H}(\cdot)$ is positive semidefinite. The Hessian matrix of $\hat{H}(\cdot)$ is calculated as follows:

$$\nabla^2 \hat{H} = \begin{bmatrix} \frac{\partial^2 \hat{H}}{\partial \mathbf{p}_1^2} & \cdots & \frac{\partial^2 \hat{H}}{\partial \mathbf{p}_1 \partial \mathbf{p}_n} \\ \vdots & \ddots & \vdots \\ \frac{\partial^2 \hat{H}}{\partial \mathbf{p}_n \partial \mathbf{p}_1} & \cdots & \frac{\partial^2 \hat{H}}{\partial \mathbf{p}_n^2} \end{bmatrix}. \quad (28)$$

According to Lemma 3, it is clear that $\frac{\partial^2 \hat{H}}{\partial \mathbf{p}_i \partial \mathbf{p}_j} = 0, \forall i \neq j$. On the other hand, similar to Lemma 4, $\frac{\partial^2 \hat{H}}{\partial \mathbf{p}_i^2}$ is calculated as follows:

$$\frac{\partial^2 \hat{H}(t)}{\partial \mathbf{p}_i^2(t)} = \int_{\mathbf{Q}} h_{\lambda}(t, R_i)\phi(\mathbf{q})d\mathbf{q}\mathbf{I}_N. \quad (29)$$

Therefore, (28) can be written as

$$\nabla^2 \hat{H}(t) = \begin{bmatrix} \alpha_1(t) \mathbf{I}_N & \dots & 0 \\ \vdots & \ddots & \vdots \\ 0 & \dots & \alpha_n(t) \mathbf{I}_N \end{bmatrix}, \quad (30)$$

where $\alpha_i(t) \triangleq \int_{\mathbf{Q}} h_{\lambda}(t, R_i) \phi(\mathbf{q}) d\mathbf{q}$, $i = 1, \dots, n$, is always positive. Hence, $\nabla^2 \hat{H}(t)$ is a positive definite matrix, and consequently a convex function. \square

The following theorem shows the convergence of agents network to the globally optimum coverage configuration using the proposed control law given by (23).

Theorem 1 (Known environment) *Assume that the density function of the environment is known and the dynamic of agents are defined by (7). If the control input of each agent is chosen as (23), then the control input of each agent converge to zero, and consequently the agents converge to the globally optimal coverage configuration, i.e. $\lim_{t \rightarrow \infty} \mathbf{p}_i(t) = \mathbf{p}_i^*$.*

Proof. Consider the following Lyapunov-like function:

$$V(t, \mathbf{P}(t)) = \hat{H}(t, \mathbf{P}(t)). \quad (31)$$

By taking the time derivative of V , it follows that:

$$\dot{V}(t, \mathbf{P}(t)) = \sum_{i=1}^n \frac{\partial \hat{H}^T(t, \mathbf{P}(t))}{\partial \mathbf{p}_i(t)} \dot{\mathbf{p}}_i(t), \quad (32)$$

Using Lemma 3, (7) and (23), we can write

$$\dot{V}(t, \mathbf{P}) = -\epsilon \sum_{i=1}^n \mathbf{W}_i^T(t) \mathbf{W}_i(t), \quad (33)$$

where $\mathbf{W}_i(t)$ is defined in (24). Similarly, taking the second-order time derivative of $V(\cdot)$ yields:

$$\begin{aligned} \ddot{V}(t, \mathbf{P}) &= \sum_{i=1}^n -2\epsilon \mathbf{W}_i^T(t) \frac{\partial \mathbf{W}_i(t)}{\partial \mathbf{p}_i(t)} \dot{\mathbf{p}}_i(t), \\ &= -2\epsilon^2 \sum_{i=1}^n \mathbf{W}_i^T(t) \frac{\partial \mathbf{W}_i(t)}{\partial \mathbf{p}_i(t)} \mathbf{W}_i(t). \end{aligned} \quad (34)$$

According to Lemma 4, $\ddot{V}(\cdot)$ is bounded, and consequently $\dot{V}(\cdot)$ is uniformly continuous [11]. Since $V(\cdot) \geq 0$ (is lower bounded) and $\dot{V}(\cdot) \leq 0$, then $V(\cdot)$ has a finite limit. Therefore, using Barbalat's lemma, $\dot{V}(\cdot) \rightarrow 0$. Considering (33) and (24), it follows that $\lim_{t \rightarrow \infty} u_i(t) = \lim_{t \rightarrow \infty} W_i(t) = 0$ and each agent converges to a point in \mathbf{Q} . Moreover, as the cost function (14) is a convex function (Lemma 5), then the gradient descent converges to the global solution [5] and hence $\lim_{t \rightarrow \infty} \mathbf{p}_i(t) = \mathbf{p}_i^*$. \square

4.2 Unknown Environment

In this section, it is supposed that the environment is unknown or equivalently $\phi(\mathbf{q})$ is priorly unknown for agents. Hence, the control input produced in the previous section can not be used directly. To remedy this problem, we propose a distributed adaptive control input such that the globally optimal coverage configuration is obtained. As shown in Fig. 2, the proposed control input of each agent consists of two layers. In the first layer, based on the

environment measurement and information received from other agents, the density function is estimated online and then using the second layer, the position of each agent is updated. In the following, we will prove that the estimated density function of each agent converges to the actual one and agents achieve globally optimal coverage configuration. For this purpose, consider following assumptions:

Assumption 1 (Mathematical model for density function) The density function $\phi(\mathbf{q})$ is represented by a basis function scheme as

$$\phi(\mathbf{q}) = \mathcal{K}^T(\mathbf{q})\mathbf{a}, \quad (35)$$

where $\mathbf{a} \in \mathbb{R}_{\geq 0}^m$ is unknown and $\mathcal{K} : \mathbf{Q} \rightarrow \mathbb{R}_{\geq 0}^m$ is known for each agent. Furthermore, $a^i \geq a_{\min}$, $i = 1, \dots, m$, and $a_{\min} \in \mathbb{R}_{> 0}$ where a^i denotes the i -th element of the vector \mathbf{a} .

Remark 3 This assumption is not limiting since any function with some smoothness requirements over a bounded domain can be approximated arbitrarily well by choosing some proper set of basis function [21].

Assumption 2 (Network connection) The network connection between agents is a connected network.

Since the parameter \mathbf{a} is unknown, each agent needs to estimate this parameter to construct its control signal. The estimated parameter \mathbf{a} and $\phi(\mathbf{q})$ by the i -th agent at time t are denoted by $\hat{\mathbf{a}}_i(t)$ and $\hat{\phi}_i(\mathbf{q}, t)$, respectively. Hence, using (35), we have

$$\hat{\phi}_i(\mathbf{q}, t) = \mathcal{K}^T(\mathbf{q})\hat{\mathbf{a}}_i(t). \quad (36)$$

It is noted that each agent can measure $\phi(\mathbf{q})$ at the current position with its sensors. In other words, $\phi(\mathbf{p}_i(t))$ is known for the i -th agent. The estimated density function error denoted by $\tilde{\phi}_i(\mathbf{q}, t)$, therefore, is calculated as

$$\tilde{\phi}_i(\mathbf{q}, t) \triangleq \hat{\phi}_i(\mathbf{q}, t) - \phi(\mathbf{q}) = \mathcal{K}^T(\mathbf{q})\tilde{\mathbf{a}}_i(t), \quad (37)$$

where $\tilde{\mathbf{a}}_i(t) \triangleq \hat{\mathbf{a}}_i(t) - \mathbf{a}$. Similar to the known environment, the same control structure is proposed, where $\phi(\mathbf{q})$ is replaced by its estimated value, $\hat{\phi}_i(\mathbf{q}, t)$, i.e.

$$\mathbf{u}_i(t) = \epsilon \int_{\mathbf{Q}} h_{\lambda}(t, R_i)(\mathbf{q} - \mathbf{p}_i(t))\hat{\phi}_i(\mathbf{q}, t)d\mathbf{q}. \quad (38)$$

As we can see from (38), the estimation of density function has a vital role in the coverage problem. As previously stated, the i -th agent can measure $\phi(\mathbf{p}_i(t))$ and hence an approximation $\hat{\phi}_i(\mathbf{q}, t)$ can be learned using sensor measurements and information shared from other agents during the agent's movement over time. For this purpose, we propose the modified version of the adaptation law introduced in [23] to update $\hat{\mathbf{a}}_i(t)$ and consequently $\hat{\phi}_i(\mathbf{q}, t)$ as follows:

$$\dot{\hat{\mathbf{a}}}_i(t) = \Gamma(\dot{\hat{\mathbf{a}}}_{\text{pre}_i}(t) - \mathbf{I}_{\text{proj}_i}(t)\dot{\hat{\mathbf{a}}}_{\text{pre}_i}(t)), \quad (39)$$

where $\Gamma \in \mathbb{R}^{m \times m}$ is a diagonal positive-definite adaptation gain matrix and $\mathbf{I}_{\text{proj}_i}(t)$ is a diagonal matrix defined as follows

$$I_{\text{proj}_i}^j(t) = \begin{cases} 0, & \text{for } \hat{a}_i^j(t) > a_{\min}, \\ 0, & \text{for } \hat{a}_i^j(t) = a_{\min}, \quad \text{and } \dot{\hat{a}}_{\text{pre}_i}^j(t) \geq 0, \\ 1, & \text{otherwise,} \end{cases} \quad (40)$$

where $I_{\text{proj}_i}^j(t)$ is the j -th diagonal element for the matrix $\mathbf{I}_{\text{proj}_i}(t)$. Furthermore, $\hat{a}_i^j(t)$ and $\dot{\hat{a}}_{\text{pre}_i}^j(t)$ are the j -th element for $\hat{\mathbf{a}}(t)$ and $\dot{\hat{\mathbf{a}}}_{\text{pre}_i}(t)$, respectively, and

$$\dot{\hat{\mathbf{a}}}_{\text{pre}_i}(t) = -\mathbf{F}_i(t)\hat{\mathbf{a}}_i(t) - \gamma(\Lambda_i(t)\hat{\mathbf{a}}_i(t) - \Upsilon_i(t)) - \zeta \sum_{j=1}^n l_{i,j}(\hat{\mathbf{a}}_i(t) - \hat{\mathbf{a}}_j(t)), \quad (41)$$

where $\gamma > 0$ is the scalar adaptation gain, $\zeta > 0$ is a consensus scalar gain, $\mathbf{F}_i(t)$ is a positive semi-definite matrix defined as:

$$\mathbf{F}_i(t) \triangleq \epsilon \int_{\mathbf{Q}} \mathcal{K}(\mathbf{q})(\mathbf{q} - \mathbf{p}_i(t))^T h_{\lambda}(t, R_i)d\mathbf{q} \int_{\mathbf{Q}} (\mathbf{q} - \mathbf{p}_i(t))\mathcal{K}^T(\mathbf{q})h_{\lambda}(t, R_i)d\mathbf{q}, \quad (42)$$

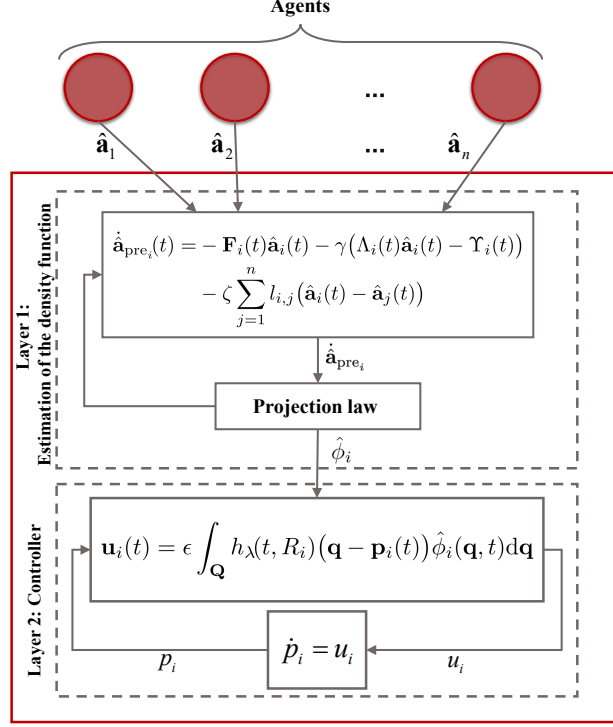


Fig. 2. Block diagram of the proposed adaptive coverage control algorithm for unknown environment.

and $\Upsilon_i(t)$ and $\Lambda_i(t)$ are defined as:

$$\Upsilon_i(t) \triangleq \int_0^t w(\tau) \mathcal{K}(\mathbf{p}_i(\tau)) \phi(\mathbf{p}_i(\tau)) d\tau, \quad (43)$$

$$\Lambda_i(t) \triangleq \int_0^t w(\tau) \mathcal{K}(\mathbf{p}_i(\tau)) \mathcal{K}^T(\mathbf{p}_i(\tau)) d\tau, \quad (44)$$

where $w(\tau)$ is a non-negative, selection-limited scalar weight function for data collection that keeps bounds on $\Lambda_i(t)$ and $\Upsilon_i(t)$. The weight $w(\tau)$ is chosen as a positive value for a certain period of time, after which its value becomes zero, i.e.

$$w(t) = \begin{cases} r, & \text{if } t < \tau_w, \\ 0, & \text{otherwise,} \end{cases} \quad (45)$$

where r is a positive value applied during time $[0, \tau_w]$.

Remark 4 *The main difference between the proposed adaptation law and the one presented in [23] is the use of $h_\lambda(\cdot)$ instead of $h_i(\cdot)$ in $\mathbf{F}_i(t)$.*

The designed adaptive coverage control algorithm is implemented in two layers. In the first phase, each agent measures $\phi(\mathbf{p}_i(t))$ in the current position, and using estimated values shared from neighboring agents provides an estimation of vector \mathbf{a} represented by $\hat{\mathbf{a}}_i(t)$. In the second phase, each agent, using its own estimated value of \mathbf{a} and (38), updates its position.

The following theorem proves that using the proposed method not only the estimated density function error tends to zero, but also agents converge to the globally optimal coverage configuration.

Theorem 2 (Unknown environment) *Under Assumption 1 and the dynamic of agents defined by (7), then the control input of each agent converge to zero, the estimated density function error of each agent tends to zero, i.e., $\lim_{t \rightarrow \infty} \tilde{\phi}_i(\mathbf{q}, t) = 0$, and, consequently, the agents converge to the globally optimal coverage configuration, i.e., $\lim_{t \rightarrow \infty} \mathbf{p}_i(t) = \mathbf{p}_i^*$.*

Proof. Consider the following Lyapunov-like function:

$$V_2(t, \mathbf{P}(t), \tilde{\mathbf{A}}(t)) = \hat{H}(t, \mathbf{P}(t)) + \frac{1}{2} \sum_{i=1}^n \tilde{\mathbf{a}}_i^T(t) \Gamma^{-1} \tilde{\mathbf{a}}_i(t). \quad (46)$$

where $\tilde{\mathbf{A}}(t) \triangleq \{\tilde{\mathbf{a}}_1(t), \dots, \tilde{\mathbf{a}}_n(t)\}$. The time derivative of $V_2(\cdot)$ is as follows

$$\dot{V}_2(\cdot) = \sum_{i=1}^n \left[\frac{\partial \hat{H}^T(t)}{\partial \mathbf{p}_i(t)} \dot{\mathbf{p}}_i(t) + \tilde{\mathbf{a}}_i^T(t) \Gamma^{-1} \dot{\tilde{\mathbf{a}}}_i(t) \right]. \quad (47)$$

Using Lemma 3, one can write

$$\dot{V}_2(\cdot) = \sum_{i=1}^n \left(- \int_{\mathbf{Q}} h_{\lambda}(t, R_i) (\mathbf{q} - \mathbf{p}_i(t))^T \phi(\mathbf{q}) d\mathbf{q} \dot{\mathbf{p}}_i(t) + \tilde{\mathbf{a}}_i^T(t) \Gamma^{-1} \dot{\tilde{\mathbf{a}}}_i(t) \right). \quad (48)$$

Substituting $\phi(\mathbf{q})$ from (37) gives:

$$\dot{V}_2(\cdot) = \sum_{i=1}^n \left[- \int_{\mathbf{Q}} h_{\lambda}(t, R_i) (\mathbf{q} - \mathbf{p}_i(t))^T \hat{\phi}_i(\mathbf{q}, t) d\mathbf{q} \dot{\mathbf{p}}_i(t) + \int_{\mathbf{Q}} h_{\lambda}(t, R_i) \tilde{\mathbf{a}}_i^T(t) \mathcal{K}(\mathbf{q}) (\mathbf{q} - \mathbf{p}_i(t))^T d\mathbf{q} \dot{\mathbf{p}}_i(t) + \tilde{\mathbf{a}}_i^T(t) \Gamma^{-1} \dot{\tilde{\mathbf{a}}}_i(t) \right]. \quad (49)$$

Substituting $\dot{\mathbf{p}}_i(t)$ from (23) yields:

$$\begin{aligned} \dot{V}_2(\cdot) = & \sum_{i=1}^n \left[- \int_{\mathbf{Q}} h_{\lambda}(t, R_i) (\mathbf{q} - \mathbf{p}_i(t))^T \hat{\phi}_i(\mathbf{q}, t) d\mathbf{q} \epsilon \int_{\mathbf{Q}} h_{\lambda}(t, R_i) (\mathbf{q} - \mathbf{p}_i(t)) \hat{\phi}_i(\mathbf{q}, t) d\mathbf{q} \right. \\ & \left. + \epsilon \int_{\mathbf{Q}} h_{\lambda}(t, R_i) \tilde{\mathbf{a}}_i^T(t) \mathcal{K}(\mathbf{q}) (\mathbf{q} - \mathbf{p}_i(t))^T d\mathbf{q} \int_{\mathbf{Q}} h_{\lambda}(t, R_i) (\mathbf{q} - \mathbf{p}_i(t)) \hat{\phi}_i(\mathbf{q}, t) d\mathbf{q} + \tilde{\mathbf{a}}_i^T(t) \Gamma^{-1} \dot{\tilde{\mathbf{a}}}_i(t) \right], \quad (50) \end{aligned}$$

Note that using (43), the second term of the right-hand side of the above equation can be rewritten as

$$\begin{aligned} & \epsilon \int_{\mathbf{Q}} h_{\lambda}(t, R_i) \tilde{\mathbf{a}}_i^T(t) \mathcal{K}(\mathbf{q}) (\mathbf{q} - \mathbf{p}_i(t))^T d\mathbf{q} \int_{\mathbf{Q}} h_{\lambda}(t, R_i) (\mathbf{q} - \mathbf{p}_i(t)) \hat{\phi}_i(\mathbf{q}, t) d\mathbf{q} \\ & = \tilde{\mathbf{a}}_i^T(t) \epsilon \int_{\mathbf{Q}} h_{\lambda}(t, R_i) \mathcal{K}(\mathbf{q}) (\mathbf{q} - \mathbf{p}_i(t))^T d\mathbf{q} \int_{\mathbf{Q}} h_{\lambda}(t, R_i) (\mathbf{q} - \mathbf{p}_i(t)) \mathcal{K}(\mathbf{q}) d\mathbf{q} \tilde{\mathbf{a}}_i^T(t) \\ & = \tilde{\mathbf{a}}_i^T(t) \mathbf{F}_i(t) \tilde{\mathbf{a}}_i(t). \quad (51) \end{aligned}$$

Using (51) and substituting $\dot{\tilde{\mathbf{a}}}_i(t)$ from (39) in the above equation gives

$$\begin{aligned} \dot{V}_2(\cdot) = & \sum_{i=1}^n \left[- \int_{\mathbf{Q}} h_{\lambda}(t, R_i) (\mathbf{q} - \mathbf{p}_i(t))^T \hat{\phi}_i(\mathbf{q}, t) d\mathbf{q} \epsilon \int_{\mathbf{Q}} h_{\lambda}(t, R_i) (\mathbf{q} - \mathbf{p}_i(t)) \hat{\phi}_i(\mathbf{q}, t) d\mathbf{q} + \tilde{\mathbf{a}}_i^T(t) \mathbf{F}_i \tilde{\mathbf{a}}_i(t) \right. \\ & \left. - \tilde{\mathbf{a}}_i^T(t) \mathbf{F}_i(t) \hat{\mathbf{a}}_i(t) - \tilde{\mathbf{a}}_i^T(t) \gamma (\Lambda_i(t) \hat{\mathbf{a}}_i(t) - \Upsilon_i(t)) - \tilde{\mathbf{a}}_i^T(t) \mathbf{I}_{\text{proj}_i}(t) \dot{\hat{\mathbf{a}}}_{\text{pre}_i}(t) \right] \\ & - \sum_{i=1}^n \tilde{\mathbf{a}}_i^T(t) \zeta \sum_{j=1}^n l_{i,j} (\hat{\mathbf{a}}_i(t) - \hat{\mathbf{a}}_j(t)). \quad (52) \end{aligned}$$

Based on (43) and (44), and the fact that $\phi(\mathbf{p}_i(\tau)) = \mathcal{K}^\top(\mathbf{p}_i(\tau))\mathbf{a}$, we have

$$\begin{aligned}
& \tilde{\mathbf{a}}_i^\top(t)\gamma(\Lambda_i(t)\hat{\mathbf{a}}_i(t) - \Upsilon_i(t)) \\
&= \tilde{\mathbf{a}}_i^\top(t)\gamma\left(\int_0^t w(\tau)\mathcal{K}(\mathbf{p}_i(\tau))\mathcal{K}^\top(\mathbf{p}_i(\tau))d\tau\hat{\mathbf{a}}_i(t) - \int_0^t w(\tau)\mathcal{K}(\mathbf{p}_i(\tau))\mathcal{K}^\top(\mathbf{p}_i(\tau))d\tau\mathbf{a}\right), \\
&= \tilde{\mathbf{a}}_i^\top(t)\gamma\left(\int_0^t w(\tau)\mathcal{K}(\mathbf{p}_i(\tau))\mathcal{K}^\top(\mathbf{p}_i(\tau))d\tau\tilde{\mathbf{a}}_i(t)\right), \\
&= \gamma\tilde{\mathbf{a}}_i^\top(t)\Lambda_i(t)\tilde{\mathbf{a}}_i(t).
\end{aligned} \tag{53}$$

Finally, using (57), we can rewrite (52) as

$$\begin{aligned}
\dot{V}_2(\cdot) &= \sum_{i=1}^n \left[-\left\| \int_{\mathbf{Q}} h_\lambda(t, R_i)(\mathbf{q} - \mathbf{p}_i(t))\hat{\phi}(\mathbf{q}, t)d\mathbf{q} \right\|^2 - \tilde{\mathbf{a}}_i^\top(t)\gamma\Lambda_i(t)\tilde{\mathbf{a}}_i(t) - \tilde{\mathbf{a}}_i^\top(t)\mathbf{I}_{\text{proj}_i}(t)\dot{\hat{\mathbf{a}}}_{\text{pre}_i}(t) \right] \\
&\quad - \sum_{i=1}^n \tilde{\mathbf{a}}_i^\top(t)\zeta \sum_{j=1}^n l_{i,j} [\hat{\mathbf{a}}_i(t) - \hat{\mathbf{a}}_j(t)].
\end{aligned} \tag{54}$$

For ease of referencing, denote the four terms in the right-hand side of (54) as $\varrho_1(t)$, $\varrho_2(t)$, $\varrho_3(t)$, and $\varrho_4(t)$, respectively. It follows that $\varrho_4(t) = -\zeta \sum_{j=1}^m \tilde{\mathbf{\Omega}}_j^\top(t)\mathbf{L}\hat{\mathbf{\Omega}}_j(t)$, where $\mathbf{\Omega}_j(t) \triangleq a^j \mathbf{1}_{n \times 1}$, $\hat{\mathbf{\Omega}}_j(t) \triangleq [\hat{a}_1^j(t), \dots, \hat{a}_n^j(t)]^\top$ and $\tilde{\mathbf{\Omega}}_j(t) \triangleq \hat{\mathbf{\Omega}}_j(t) - \mathbf{\Omega}_j(t)$. Based on the properties of the Laplacian matrix \mathbf{L} , $\mathbf{\Omega}_j^\top \mathbf{L} = a^j \mathbf{1}_{n \times 1}^\top \mathbf{L} = 0, \forall j$. Therefore,

$$-\zeta \sum_{j=1}^m \tilde{\mathbf{\Omega}}_j^\top(t)\mathbf{L}\hat{\mathbf{\Omega}}_j(t) = -\zeta \sum_{j=1}^m \hat{\mathbf{\Omega}}_j^\top(t)\mathbf{L}\hat{\mathbf{\Omega}}_j(t). \tag{55}$$

It is clear that $\varrho_1(t) \leq 0$, and according to the definition of $w(t)$ and \mathbf{L} , $\varrho_2(t)$ and $\varrho_4(t)$ are also non-positive. Using (40), if $\hat{a}_i^j(t) > a_{\min}$ or $\hat{a}_i^j(t) = a_{\min}$ and $\dot{\hat{a}}_{\text{pre}_i}^j(t) \geq 0$, then $\mathbf{I}_{\text{proj}_i}^j(t) = 0$, and the corresponding term is vanished. On the other hand, if $\hat{a}_i^j(t) = a_{\min}$ and $\dot{\hat{a}}_{\text{pre}_i}^j(t) < 0$, then $\mathbf{I}_{\text{proj}_i}^j(t) = 1$ and we observe that $\tilde{a}_i^j(t) = \hat{a}_i^j(t) - a^j \leq 0$, since $a^j \geq a_{\min}$. Therefore, $\varrho_3(t) \leq 0$, and, consequently, $\dot{V}_2(\cdot) \leq 0$. It can be shown that $\ddot{V}_2(\cdot)$ is bounded and $\dot{V}_2(\cdot)$ is therefore uniformly continuous. Since $V_2(\cdot) \geq 0$ (is lower bounded) and $\dot{V}_2(\cdot) \leq 0$, then $V_2(\cdot)$ has a finite limit. Therefore, using Barbalat's lemma, $\dot{V}_2(\cdot) \rightarrow 0$, and as a result $\varrho_i(t) \rightarrow 0, i = 1, \dots, 4$. Hence it follows that:

$$\lim_{t \rightarrow \infty} \int_{\mathbf{Q}} h_\lambda(t, R_i(\mathbf{q}, \mathbf{P}(t)))(\mathbf{q} - \mathbf{p}_i(t))\hat{\phi}_i(\mathbf{q}, t)d\mathbf{q} = 0. \tag{56}$$

Furthermore, using (37), it follows that $\lim_{t \rightarrow \infty} \tilde{\phi}_i(\mathbf{q}, t) = 0$. Note that the control input $\mathbf{u}_i(t)$ given by (38) can be written as

$$\mathbf{u}_i(t) = -\epsilon \frac{\partial \tilde{H}(t)}{\partial \mathbf{p}_i(t)}, \quad i = 1, \dots, n, \tag{57}$$

where

$$\tilde{H}(t, \mathbf{P}(t)) \triangleq \frac{1}{2} \sum_{i=1}^n \int_{\mathbf{Q}} h_\lambda(t, R_i) \|\mathbf{q} - \mathbf{p}_i(t)\|^2 \hat{\phi}_i(\mathbf{q}, t) d\mathbf{q}. \tag{58}$$

Similar to Lemma 5, we can show that $\tilde{H}(\cdot)$ is a convex function. Therefore, using (38), the global minimum of $\tilde{H}(\cdot)$ is obtained. Since $\hat{\phi}_i(\mathbf{q}, t) \rightarrow \phi(\mathbf{q})$ as $t \rightarrow \infty$, then $\tilde{H}(\cdot) \rightarrow \hat{H}(\cdot)$ as $t \rightarrow \infty$. Hence, using Lemma 2, $\lim_{t \rightarrow \infty} \mathbf{p}_i(t) = \mathbf{p}_i^*$ is obtained. \square

5 Simulation Results

In this section, the simulation results of the proposed coverage method in known and unknown environments are presented. In order to evaluate the effectiveness of the proposed method, various scenarios are conducted.

Table 2

Parameters of the proposed method for simulation scenarios of the known environment.

Parameter	ϵ	λ_f	λ_s	α	ρ_{trunc}
Value	0.1	2×10^{-3}	4	25×10^{-3}	0.2

Furthermore, to show the performance of the proposed method in comparison with other approaches, the proposed method is compared with presented methods in [7] and [23] in known and unknown environments, respectively, based on the cost function given by (5). It should be noted that, the initial position of agents in comparative studies is considered to be the same. The video of all scenarios is available through this link: <https://www.youtube.com/watch?v=6QcD1WQSBZY>. The following assumptions are considered in this section:

- The density function of the environment is parameterized based on Assumption 1 and with the help of 25 truncated Gaussian functions (i.e. $\mathcal{K}(\mathbf{q}) = [\mathcal{K}_1(\mathbf{q}), \dots, \mathcal{K}_{25}(\mathbf{q})]^T$) as follows:

$$\mathcal{K}_j(\mathbf{q}) \triangleq \begin{cases} G_j(\mathbf{q}) - G_{\text{trunc}}, & \text{if } \|\mathbf{q} - \mu_j\| < \rho_{\text{trunc}}, \\ 0, & \text{otherwise,} \end{cases} \quad (59)$$

where

$$G_j(\mathbf{q}) \triangleq \frac{1}{\sigma\sqrt{2\pi}} \exp\left\{-\frac{\|\mathbf{q} - \mu_j\|^2}{2\sigma^2}\right\}, \quad (60)$$

$$G_{\text{trunc}} \triangleq \frac{1}{\sigma\sqrt{2\pi}} \exp\left\{-\frac{\rho_{\text{trunc}}^2}{2\sigma^2}\right\}, \quad (61)$$

and μ_j is the mean of G_j and σ is the standard deviation of Gaussian functions. The parameter ρ_{trunc} is the radius of a circle to the center of μ_j .

- The environment \mathbf{Q} is taken to be a unit square and it is divided into an even 5×5 grid. Each truncated Gaussian mean μ_j is set so that each of 25 Gaussian functions is centered at its corresponding grid square.
- To ensure a fair comparison between the performance of our algorithm and the Voronoi method, the control gains ϵ and k_{prop} are regulated so that both algorithms operate within the same control input range.
- For implementation purposes, the algorithm is discretized with a sampling time of 0.01s.

5.1 Known environments

In this subsection, three scenarios are conducted in the known environment to evaluate the performance of the proposed method compared to the Voronoi-based method in [7]. The detailed information of the selected parameters for these scenarios are given in TABLE 2.

In the first two scenarios, we assume that the density function of the environment remains the same, but we vary the initial agent configurations. The objective is to compare the performance of the proposed method with the Voronoi-based method. To achieve this goal, we have chosen to employ a total of fourteen agents, and the vector \mathbf{a} is considered as

$$\mathbf{a}_{25 \times 1} \triangleq \begin{cases} a^j = 29960, & \text{for } j = 7 \text{ and } j = 9, \\ a^j = 50, & \text{otherwise.} \end{cases} \quad (62)$$

Note that based on TABLE 2 and this selection of the vector \mathbf{a} , we have $\phi(\mathbf{q}) \neq 0, \forall \mathbf{q} \in \mathbf{Q}$, which means there is no zero information area in the environment. The results of these simulation scenarios are shown in Fig. 3, and Fig. 4. As can be seen in Fig. 3(d), and Fig. 4(d), it is clear that the cost generated by the proposed algorithm is lower than the Voronoi-based method given by [7]. In addition, as observed in Fig. 3(b), and Fig. 4(b), owing to the global optimality of the proposed method, the final configuration obtained by the proposed method are identical for both the first and second scenarios, therefore, our algorithm is not sensitive to the initial configuration of the agents. In contrast, as can be seen from Fig. 3(c), and Fig. 4(c), when the initial condition of the agents changed, the Voronoi algorithm converged to two different final configuration. This is resulted from the dependency of this algorithm to the initial configuration of agents and its locally optimal nature. Moreover, by comparing Fig. 3(b) and Fig. 4(b), with Fig. 3(c) and Fig. 4(c), the proposed method clearly distributes the agents in the regions with more information than the Voronoi-based method.

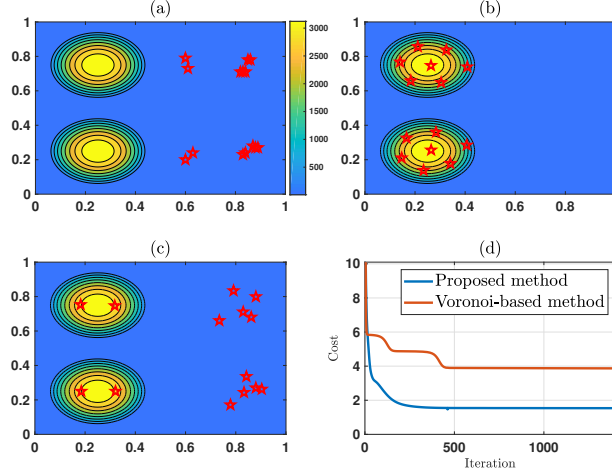


Fig. 3. Simulation results of the first scenario for known environment with no zero information area: (a) Initial configuration of the agents. (b) Final configuration using the proposed method. (c) Final configuration using the Voronoi-based method [7]. (d) The value of the cost function at each step.

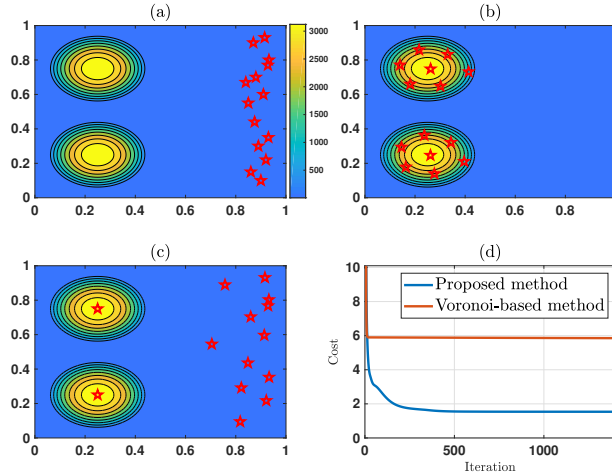


Fig. 4. Simulation results of the second scenario for known environment with no zero information area: (a) Initial configuration of the agents. (b) Final configuration using the proposed method. (c) Final configuration using the Voronoi-based method [7]. (d) The value of the cost function at each step.

In the third scenario, the performance of the proposed method is investigated in the environment with separated information areas. For this purpose, two separated information areas are modeled using the following vector \mathbf{a} :

$$\mathbf{a}_{25 \times 1} \triangleq \begin{cases} a^j = 29960, & \text{for } j = 7 \text{ and } j = 9, \\ a^j = 0, & \text{otherwise.} \end{cases} \quad (63)$$

The proposed method, as shown in Fig. 5(c), distributes agents across two regions with higher density functions, while the Voronoi-based method introduced by [7] places most of the agents in a area with zero density function. Clearly, as shown in Fig. 5(d), the cost generated by the proposed method is much less than the Voronoi-based method. The results of the considered scenarios show that the proposed method effectively distributes agents in the environment, and creates a low cost compared to the Voronoi-based method.

5.2 Unknown environments

In this subsection, the performance of the proposed method in comparison with the Voronoi-based method introduced by [23] in an unknown environment with separated information areas is investigated. For this purpose, two separated

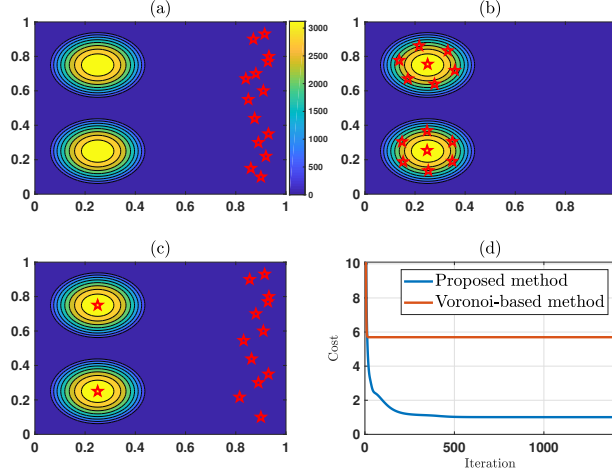


Fig. 5. Simulation results of the third scenario for known environment containing separated information areas: (a) Initial configuration of the agents. (b) Final configuration using the proposed method. (c) Final configuration using the Voronoi-based method [7]. (d) The value of the cost function at each step.

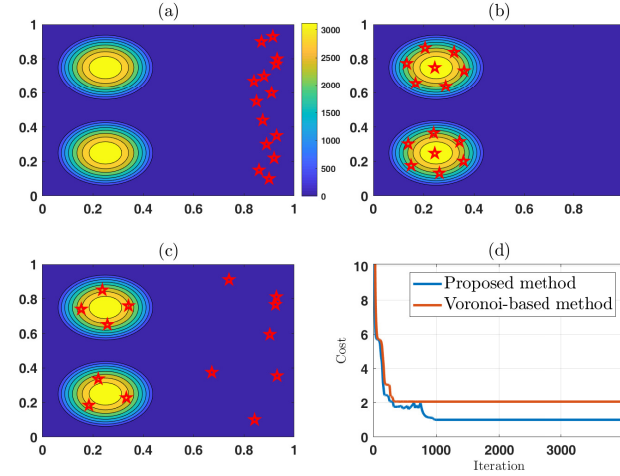


Fig. 6. Simulation results of scenario for unknown environment containing separated information areas: (a) Initial configuration of the agents. (b) Final configuration using the proposed method. (c) Final configuration using the Voronoi-based method [23]. (d) The value of the cost function at each step.

Table 3

Parameters of the proposed method for simulation scenario of the unknown environment.

Parameter	γ	ζ	$l_{i,j}$	ϵ	w	$\hat{\mathbf{a}}_{i_{\text{initial}}}$	\mathbf{a}_{min}	ρ_{trunc}
Value	0.14	0.01	1	0.9	180	$400 \times \mathbf{1}_{25 \times 1}$	$\mathbf{0}_{25 \times 1}$	0.2

information areas modeled by (63) are considered. The detailed information of the parameters of the proposed method in these scenarios are given in TABLE 3. The initial configuration of agents is shown in Fig. 6(a).

Note that, in order to facilitate the learning the information distribution in the environment, the centered Gaussian peaks in all cells are initially assumed to be the same. This causes the agents to have a tendency to cover all regions and spread evenly throughout the environment, resulting in better learning. This is the reason why the Voronoi algorithm performs better in the unknown environment compared to the third scenario. In this case, the agents initially assume that there is information distributed throughout the environment, prompting them to move. These movements prevent the agents from getting stuck in zero information areas. Moreover, unlike the known scenarios where $\lambda(\cdot)$ started from a higher value and monotonically decreased, here we start with a relatively low value for $\lambda(\cdot)$ in the early stages and gradually increase it until the agents have learned the environment, as indicated by a

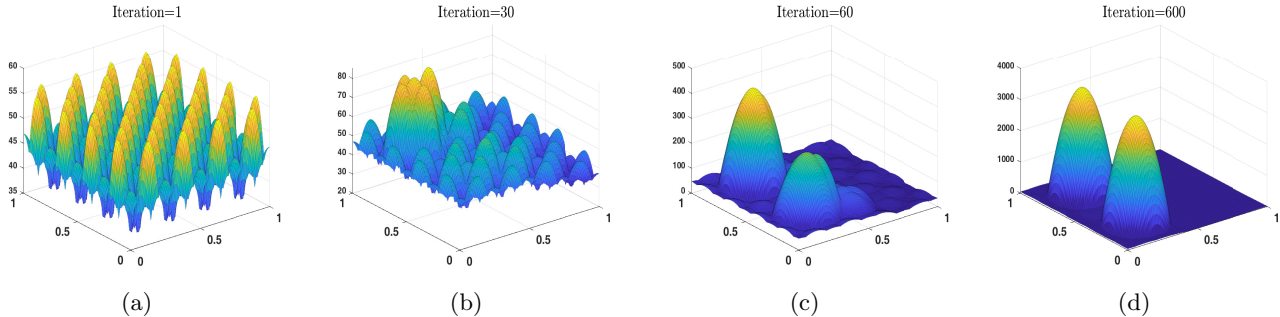


Fig. 7. Environment estimation in iterations 1, 30, 60 and 600 are shown in figures (a), (b), (c) and (d) respectively.

small relative change in $\hat{\mathbf{a}}$. The formula for the relative change in the objective function (RCOV) value is defined as follows:

$$RCOV = \frac{|f(x_{k+1}) - f(x_k)|}{|f(x_k)|} \times 100\%, \quad (64)$$

where $f(x_k)$ is the value of the objective function at the k -th iteration. Once a threshold of 1% is reached, we allow $\lambda(\cdot)$ to decrease monotonically, similar to the known scenarios. This prevents the agents from concentrating in the center of information in the early stages and allows them to spread and learn the environment more effectively.

The simulated results of the proposed method and the Voronoi-based method are shown in Fig. 6(b) and Fig. 6(c), respectively. It is clear that the proposed method is effectively distributed the agents among the information areas compared to the Voronoi-based method. The final cost value of the proposed method, as shown in Fig. 6(d), is lower than the Voronoi-based method. In addition, the estimated density function of the environment in different iterations is shown in Fig. 7. It is worth highlighting that, since the density function of the environment in the third and the current scenario is assumed to be the same, the final configuration and cost in these scenarios remain identical when using the proposed method. This outcome is a direct result of global nature of the solutions derived through our method.

5.3 Discussion

This section provides a comprehensive discussion by exploring key aspects, including computational complexity, convergence rate, and path length, to assess the algorithm's efficiency, effectiveness, and suitability for various real-world applications. Finally, to conclude our examination, we investigate the limitations encountered and discuss future research directions.

5.3.1 Complexity analysis

In this section, we delve into the computational complexity of our proposed algorithm, comparing it to that of the Voronoi coverage algorithm. It is worth noting that, for implementation purposes, we consider the discrete form of (8) where the environment Q is discretized into N points.

In the Voronoi coverage algorithm, the primary computation of the discrete control signal entails two main steps. First, there is a summation over all points in set Q , and then the computation of $h_i(\cdot)$ values. Calculating $h_i(\cdot)$ involves computing the distance from the point q to all n agents, which amounts to order n operation, and comparing these distances between the current agent and the point to all other computed distances to determine the value of $h_i(\cdot)$, which involves $n - 1$ comparisons. This results in a computation of complexity order $N(2n - 1)$. Given that $N \gg 2n - 1$, the complexity of this algorithm can be expressed as $\mathcal{O}(N)$.

Likewise the computational complexity of our proposed method depends on a summation over all points in set Q . However, we need to deal with $h_\lambda(\cdot)$ instead of $h_i(\cdot)$. Similar to $h_i(\cdot)$, computing the values for $h_\lambda(\cdot)$ requires us to initially determine the distance from point q to all n agents, which amounts to order n operation. However, when constructing the ranking function (12), we employ a Quicksort algorithm as described in [8, 15], which in its worst-case scenario results in a complexity order of $n \log(n)$. Therefore, the complexity of our algorithm will be of order $N(n \log(n) + n)$. Given that $N \gg n(\log(n) + 1)$, the computational complexity of our algorithm can also be expressed as $\mathcal{O}(N)$. Therefore, both algorithms exhibit the same order of computational complexity.

Table 4

The number of iterations required for convergence in scenario 3 for various ϵ values

ϵ	0.10	0.13	0.15	0.2	0.3
Number of Iteration	235	40	30	28	20

Table 5

The length of the path taken by all agents in each scenario for the first 1400 iterations.

	Known Environment			Unknown
	Scenario 1	Scenario 2	Scenario 3	Environment
Voronoi Method	1.6	1.3	1.1	5.2
Proposed Method	8.3	9.7	9.6	12.5

5.3.2 Input range and convergence rate

Another important consideration is the convergence rate of the algorithm, which plays a pivotal role in assessing its efficiency and practicality. The convergence rate of the algorithm is closely tied to the input range within which the agents operate. In our approach, the amplitude range of the control signal can be flexibly adjusted by modifying a positive scalar value, denoted as ϵ . This scalar serves as a gain factor that directly influences the input range for the agents. Specifically, choosing higher values of ϵ expands the range of permissible control inputs, allowing the agents to adjust their positions more rapidly in response to changing conditions.

To illustrate this fact, the RCOV given by (64) is used as a metric to measure the convergence of our algorithm. In this work, a threshold of 0.1% is employed below which the algorithm is considered to have converged. TABLE 4 shows the the number of iterations required for our algorithm to converge for various values of ϵ in the third scenario. As can be seen from TABLE 4, higher gain values effectively accelerate the convergence of the algorithm. However, it is crucial to note that the choice of gain ϵ should be made carefully to ensure that agents remain within the convex environment. This constraint is necessary to facilitate the minimization of the cost function.

5.3.3 Path length

An essential factor in coverage control is the length of the path that agents traverse within an environment. To evaluate this parameter, we introduce the following index

$$l_p = \sum_{i=1}^n \sum_{k=0}^{N_s} \|\mathbf{p}_i(k+1) - \mathbf{p}_i(k)\|, \quad (65)$$

where N_s denotes the number of simulation steps and l_p is the length taken by all agents. In TABLE 5, the path lengths traveled by all agents in various scenarios using different algorithms are presented. As demonstrated in TABLE 5, the path length taken by agents utilizing our algorithm is longer than the l_p distance of the Voronoi algorithm. This is because our algorithm ensures agents reach their final optimal positions, whereas the Voronoi method may encounter instances of getting stuck midway through the optimization process. It is also worth noting that in the third scenario where the environment is known, the l_p distance is less than the path length in the unknown environment scenario. This distinction arises because in the unknown environment scenario, the environment is unknown to the agents. Consequently, the agents not only need to explore and identify the environment but also navigate to positions with a higher density of data. Therefore, the path length in scenarios where the environment is unknown to the agents is generally longer compared to scenarios with known environments.

5.3.4 Limitations and future works

This work exclusively deals with a simplified representation of agents, considering them as point entities characterized by single integrator dynamics. We have not accounted for the agents' specific longitudinal and lateral dimensions in this work. Additionally, we have assumed that these agents are holonomic, meaning they can move freely in any direction without any constraints. Moreover, the environment is assumed to be obstacle-free.

However, there are several avenues for future research in this field. Firstly, researchers can delve into more complex vehicle dynamics, considering real-world scenarios where agents may have specific sizes and limitations in their

movements, such as non-holonomic constraints. This would lead to a more accurate modeling of the agents' behavior in practical situations.

Secondly, addressing the coverage problem in environments containing obstacles presents an intriguing challenge. In many real-world applications, agents must navigate around obstacles to effectively cover the entire area of interest. Investigating strategies and algorithms that allow agents to intelligently avoid obstacles while optimizing coverage could significantly advance this field of research.

6 Conclusion

In this work, we have introduced a novel approach to tackle the challenges associated with coverage control in multi-agent systems. Our approach offers a comprehensive solution that not only ensures global optimality in agent configuration but also effectively addresses the issue of agents becoming stationary in regions lacking information. The unique metric employed in our approach progressively aligns with the conventional Voronoi-based cost function over time, leading to enhanced performance. Theoretical analyses demonstrate the asymptotic convergence of agents towards an optimal configuration. Furthermore, our technique proves to be highly adaptive, suitable for a wide range of environments, including those with both known and unknown information distributions. Finally, through rigorous simulations, we have showcased the efficacy of our proposed method, comparing it with Voronoi-based algorithms, and highlighting its superior performance.

References

- [1] Farshid Abbasi, Afshin Mesbahi, and Javad Mohammadpour Velni. Coverage control of moving sensor networks with multiple regions of interest. In *2017 American Control Conference (ACC)*, pages 3587–3592. IEEE, 2017.
- [2] Farshid Abbasi, Afshin Mesbahi, and Javad Mohammadpour Velni. A team-based approach for coverage control of moving sensor networks. *Automatica*, 81:342–349, 2017.
- [3] Rihab Abdul Razak, Sukumar Srikant, and Hoam Chung. Decentralized and adaptive control of multiple nonholonomic robots for sensing coverage. *International Journal of Robust and Nonlinear Control*, 28(6):2636–2650, 2018.
- [4] Alessia Benevento, María Santos, Giuseppe Notarstefano, Kamran Paynabar, Matthieu Bloch, and Magnus Egerstedt. Multi-robot coordination for estimation and coverage of unknown spatial fields. In *IEEE International Conference on Robotics and Automation (ICRA)*, pages 7740–7746, 2020.
- [5] Stephen P Boyd and Lieven Vandenberghe. *Convex optimization*. Cambridge university press, 2004.
- [6] Andrea Carron and Melanie N Zeilinger. Model predictive coverage control. *IFAC-PapersOnLine*, 53(2):6107–6112, 2020.
- [7] Jorge Cortes, Sonia Martinez, Timur Karatas, and Francesco Bullo. Coverage control for mobile sensing networks. *IEEE Transactions on robotics and Automation*, 20(2):243–255, 2004.
- [8] Charles AR Hoare. Quicksort. *The computer journal*, 5(1):10–16, 1962.
- [9] Katharin R Jensen-Nau, Tucker Hermans, and Kam K Leang. Near-optimal area-coverage path planning of energy-constrained aerial robots with application in autonomous environmental monitoring. *IEEE Transactions on Automation Science and Engineering*, 2020.
- [10] Yiannis Kantaros, Michalis Thanou, and Anthony Tzes. Distributed coverage control for concave areas by a heterogeneous robot-swarm with visibility sensing constraints. *Automatica*, 53:195–207, 2015.
- [11] Hassan K Khalil. *Nonlinear systems*, volume 115. 2002.
- [12] Liya Li, Peng Shi, and Choon Ki Ahn. Distributed iterative fir consensus filter for multiagent systems over sensor networks. *IEEE Transactions on Cybernetics*, 52(6):4647–4660, 2020.
- [13] Xiaojie Li, Peng Shi, Yiguang Wang, and Shuoyu Wang. Cooperative tracking control of heterogeneous mixed-order multiagent systems with higher-order nonlinear dynamics. *IEEE Transactions on Cybernetics*, 52(6):5498–5507, 2020.
- [14] Haifeng Ling, Tao Zhu, Weixiong He, Hongchuan Luo, Qing Wang, and Yi Jiang. Coverage optimization of sensors under multiple constraints using the improved PSO algorithm. *Mathematical Problems in Engineering*, 2020.
- [15] Conrado Martínez and Salvador Roura. Optimal sampling strategies in quicksort and quickselect. *SIAM Journal on Computing*, 31(3):683–705, 2001.
- [16] Shaofeng Meng and Zhen Kan. Deep reinforcement learning-based effective coverage control with connectivity constraints. *IEEE Control Systems Letters*, 6:283–288, 2021.
- [17] Junkang Ni, Peng Shi, Yu Zhao, Quan Pan, and Shuoyu Wang. Fixed-time event-triggered output consensus tracking of high-order multiagent systems under directed interaction graphs. *IEEE Transactions on Cybernetics*, 52(7):6391–6405, 2020.
- [18] DongKi Noh, WooJu Lee, Hyoung-Rock Kim, Il-Soo Cho, In-Bo Shim, and SeungMin Baek. Adaptive coverage path planning policy for a cleaning robot with deep reinforcement learning. In *2022 IEEE International Conference on Consumer Electronics (ICCE)*, pages 1–6. IEEE, 2022.

- [19] Huy X Pham, Hung M La, David Feil-Seifer, and Matthew Deans. A distributed control framework for a team of unmanned aerial vehicles for dynamic wildfire tracking. In *2017 IEEE/RSJ International Conference on Intelligent Robots and Systems (IROS)*, pages 6648–6653. IEEE, 2017.
- [20] Erick J Rodríguez-Seda, Xiaotian Xu, Josep M Olm, Arnau Dòria-Cerezo, and Yancy Diaz-Mercado. Self-triggered coverage control for mobile sensors. *IEEE Transactions on Robotics*, 2022.
- [21] Robert M Sanner and Jean-Jacques E Slotine. Gaussian networks for direct adaptive control. In *1991 American control conference*, pages 2153–2159. IEEE, 1991.
- [22] Mac Schwager, Francesco Bullo, David Skelly, and Daniela Rus. A ladybug exploration strategy for distributed adaptive coverage control. In *2008 IEEE International Conference on Robotics and Automation*, pages 2346–2353. IEEE, 2008.
- [23] Mac Schwager, Daniela Rus, and Jean-Jacques Slotine. Decentralized, adaptive coverage control for networked robots. *The International Journal of Robotics Research*, 28(3):357–375, 2009.
- [24] Mac Schwager, Michael P Vitus, Samantha Powers, Daniela Rus, and Claire J Tomlin. Robust adaptive coverage control for robotic sensor networks. *IEEE Transactions on Control of Network Systems*, 4(3):462–476, 2015.
- [25] Rutuja Shivgan and Ziqian Dong. Energy-efficient drone coverage path planning using genetic algorithm. In *2020 IEEE 21st International Conference on High Performance Switching and Routing (HPSR)*, pages 1–6. IEEE, 2020.
- [26] Daniel E Soltero, Mac Schwager, and Daniela Rus. Decentralized path planning for coverage tasks using gradient descent adaptive control. *The International Journal of Robotics Research*, 33(3):401–425, 2014.
- [27] Cheng Song and Yuan Fan. Coverage control for mobile sensor networks with limited communication ranges on a circle. *Automatica*, 92:155–161, 2018.
- [28] Cheng Song, Lu Liu, Gang Feng, Yuan Fan, and Shengyuan Xu. Coverage control for heterogeneous mobile sensor networks with bounded position measurement errors. *Automatica*, 120:109118, 2020.
- [29] Bing Sun, Daqi Zhu, Chen Tian, and Chaomin Luo. Complete coverage autonomous underwater vehicles path planning based on gladius bio-inspired neural network algorithm for discrete and centralized programming. *IEEE Transactions on Cognitive and Developmental Systems*, 11(1):73–84, 2018.
- [30] Chuangchuang Sun, Shirantha Welikala, and Christos G Cassandras. Optimal composition of heterogeneous multi-agent teams for coverage problems with performance bound guarantees. *Automatica*, 117:108961, 2020.
- [31] Qihai Sun, Ming Chi, Zhi-Wei Liu, and Dingxin He. Observer-based coverage control of unicycle mobile robot network in dynamic environment. *Journal of the Franklin Institute*, 2022.
- [32] Qihai Sun, Tianjun Liao, Zhi-Wei Liu, Ming Chi, and Dingxin He. Fixed-time coverage control of mobile robot networks considering the time cost metric. *Sensors*, 22(22):8938, 2022.
- [33] Yuxing Yang, Mao Su, Huijin Fan, Lei Liu, and Bo Wang. A constructive density function path leading to global coverage strategy for a gaussian random field. In *2023 IEEE 12th Data Driven Control and Learning Systems Conference (DDCLS)*, pages 249–254. IEEE, 2023.
- [34] Dengxiu Yu, Hao Xu, CL Philip Chen, Wenjie Bai, and Zhen Wang. Dynamic coverage control based on k-means. *IEEE Transactions on Industrial Electronics*, 69(5):5333–5341, 2021.
- [35] Daqi Zhu, Chen Tian, Bing Sun, and Chaomin Luo. Complete coverage path planning of autonomous underwater vehicle based on GBNN algorithm. *Journal of Intelligent & Robotic Systems*, 94(1):237–249, 2019.
- [36] Lei Zuo, Yang Shi, and Weisheng Yan. Dynamic coverage control in a time-varying environment using bayesian prediction. *IEEE transactions on cybernetics*, 49(1):354–362, 2017.
- [37] Lei Zuo, Weisheng Yan, and Maode Yan. Efficient coverage algorithm for mobile sensor network with unknown density function. *IET Control Theory & Applications*, 11(6):791–798, 2017.